Spatiotemporal Patterns in Thermokinetic Models of Cross-Flow Reactors

Olga Nekhamkina, Boris Y. Rubinstein, and Moshe Sheintuch
Dept. of Chemical Engineering, Technion Israel Institute of Technology, Haifa 32 000, Israel

The behavior of stationary and moving spatially-periodic patterns in a simple cross-flow reactor was simulated and analyzed for a situation in which reactant is supplied continuously along the reactor and a first-order exothermic reactor occurs. The Danckwerts boundary conditions for realistic Le and Pe values. While the unbounded (infinitely long) reactor is an asymptotic case used to study the stability of the homogeneous solution, the moving waves that emerge in the convectively unstable unbounded system may be arrested at the boundaries of a bounded system and stationary waves are established above some amplification threshold. Sustained periodic and aperiodic behavior may emerge under certain conditions. The spatial behavior in the bounded system with $Pe \to \infty$ is analogous to the temporal behavior of the simple thermokinetic CSTR problem and the behavior of the distributed system is classified according to that of the lumped one.

Introduction

Dispersion of a reactant along a packed-bed reactor, rather than supplying it with the feed, may be advantageous in several classes of reactions: Gradual feeding of oxygen may improve selectivity in partial-oxidation reactions (Tèllez et al., 1999) where high feed concentration leads to poor selectivity, while low concentration limits the rate and conversion. By dispersing the feed along the reactor in reactions with self-inhibition (typically described by Langmuir-Hinshelwood kinetics), we may maintain the reactant concentration at its optimal concentration, a value that leads to a maximal rate (Sheintuch et al., 1986; Westerterp et al., 1984). Such a supply can be fixed at discrete ports or, with the help of selective membranes which are currently a subject of intensive investigation, distributed continuously along the reactor. A continuous supply of a reactant may be effectively achieved for a second reaction in a sequence of two consecutive reactions, when the first one is reacting at an almost constant rate.

The classes of reactions described above, like partial or complete oxidation and hydrogenation, are highly exothermic and activated, and often exhibit reactant self-inhibition. Enthalpy must be removed continuously in these units. The technical incorporation of mass-supply and heat removal is a challenging technical problem, as it requires two interfaces within the reactor. These can be organized as an annular tube with mass transfer at one wall and heat transfer at the other. Another possibility is a multitube reactor incorporating two kinds of tubes for the two transfer processes. The latter is, probably, a more practical approach, while the former is a good model for describing the process. Radial gradients are expected in either case, but we will ignore them here and describe the problem as one-dimensional (1-D). The unique aspect of such a reactor is that, sufficiently far from the inlet, the system approaches a homogeneous (space-independent) solution, which should be derived from certain optimization considerations. Highly-exothermic or highly-activated reactions may yield such multiple solutions, and in the distributed system fronts separating different states may be formed.

The purpose of this work is to analyze the rich plethora of spatiotemporal patterns, including standing or moving waves and aperiodic patterns, that may emerge in such a system. Several recent works have pointed out that patterns may be induced by the interaction of kinetics and convection. These patterns are different from the Turing structures (Turing,

Correspondence concerning this article should be addressed to M. Sheintuch.

1952) when the inhibitor diffuses sufficiently faster than the activator.

The convection-reaction patterns are intriguing academically and may be of importance for design and operation of commercial reactors. Previous works of such patterns analyzed models with ''learning kinetics'' like the Brusselator, or used boundary conditions that do not correspond to any actual situation. The present work analyzes patterns due to a first-order exothermic reaction with realistic parameters ($Le \gg 1$, $Pe \gg 1$) and realistic (Danckwerts) boundary-conditions. Yakhnin et al. (1994a,b; 1995) in their investigation of the differential flow induced chemical instability (DIFICI), applied linear stability analysis to reactors with periodic boundary conditions (''ring-shaped'' reactor) or to ''linear'' reactors with special boundary conditions that maintain the homogeneous solution. Patterns emerge when the magnitude of the differential bulk flow exceeds a critical value. They simulated traveling wave trains in a system with periodic boundary conditions, and followed the amplification of perturbations in a ''linear'' system with Danckwerts conditions. In all their studies the calculations were carried out for the range of parameters that correspond to convectively unstable, but absolutely stable, systems (defined later). They did not simulate stationary patterns. Moving patterns due to the interaction of thermal bistability and feed dispersion along the reactor were suggested by us (Shvartsman and Sheintuch, 1995). Stationary space-periodic structures in a Brusselator were studied by Kuznetsov et al. (1997), and Andresén et al. (1999). Finally, the authors (Nekhamkina et al., 2000) have recently conducted a weak nonlinear analysis of a thermokinetic model of a catalytic reactor.

This work extends a series of previous articles on the dynamics of the fixed-bed reactor, in which we studied spatiotemporal patterns in heterogeneous (Barto and Sheintuch, 1994) and homogeneous (Sheintuch and Nekhamkina, 1999) models using the generic first-order Arrhenius kinetics, or a detailed multistep model, like the one that applies to CO oxidation in the catalytic converter (Keren and Sheintuch, 2000). In all the models cited above patterns emerge due to interaction of kinetics or thermal bistability with a slow reversible change in activity. In the present model, however, the activity is held constant and patterns emerge due to the interaction of enthalpy and mass balances. Oscillatory or even chaotic behavior may emerge due to the interaction of the front-motion upstream and flow downstream. It can be described by a single-variable integro-differential equation suggesting that complex dynamics may result in distributed systems from simple kinetics that admit simple bistability in a mixed system. Recently, Lauschke and Gilles, (1994) and Hua et al. (1998) analyzed and observed complex dynamics in a loop-reactor heat exchanger using a reaction with simple bistable kinetics.

In spatially extended systems with convection, like fixed-bed reactors, instabilities are referred to as either ''convective'' or as ''absolute'', when disturbances spread at velocities that are smaller or larger then the fluid velocity, respectively. In convectively unstable, but absolutely stable, bounded systems the amplified perturbations are ultimately swept out of the system leaving the reactor in its stationary state. Thus, perturbations cannot be sustained. A convectively unstable system may be made absolutely unstable by introducing a spatial feedback loop, for example, if the outlet stream is partially recycled. Thus, the boundary conditions are of considerable importance for the stability of the system.

In the present work we simulate and analyze the behavior of stationary spatially-periodic patterns in a ''linear'' reactor with Danckwerts boundary conditions and realistic Le and Pe values. We find that the moving waves that emerge in the convectively unstable unbounded system are usually arrested at the boundaries, and stationary waves are established above some amplification threshold (Nekhamkina et al. 2000). Sustained periodic and aperiodic behavior may emerge under certain conditions. We also draw the analogy between the distributed system and the simple CSTR problem. These results may lead to new design or operation procedures of catalytic reactors, and join the growing family of spatially-patterned reactors, like the reactor with flow-reversal or the loop-reactor. The observed behavior is also different than previous studies of patterns in convection-reaction system in that the underlying mechanism does not require oscillatory kinetics (that is, Hopf bifurcation), or different diffusivities (Turing bifurcation) or even differential bulk flow.

Reactor Models and Linear Analysis

The homogeneous model of catalytic reactors assumes that interphase gradients of temperature and concentration between the fluid and solid phases are absent. The mass and energy balances are conventional ones except for the mass supply term; they account for accumulation, convection, axial dispersion, chemical reaction $r(C, T)$, heat loss due to cooling ($S_T = \alpha_T(T - T_w)$) and mass supply through a membrane wall ($S_C = \alpha_C(C - C_w)$). For the 1-D case, the appropriate system equation has the following form

$$\frac{\partial C}{\partial t} + u\frac{\partial C}{\partial z} - \epsilon D_f \frac{\partial^2 C}{\partial z^2} = -(1-\epsilon)r(C,T) + S_C,$$

$$(\rho c_p)_e \frac{\partial T}{\partial t} + (\rho c_p)_f u\frac{\partial T}{\partial z} - k_e \frac{\partial^2 T}{\partial z^2} = (-\Delta H)(1-\epsilon)r(C,T) + S_T, \quad (1)$$

The Danckwerts boundary conditions are typically imposed on the model

$$z = 0,\ \epsilon D_f \frac{\partial C}{\partial z} = u(C - C_{\text{in}}), \quad k_e \frac{\partial T}{\partial z} = (\rho c_p)_f u(T - T_{\text{in}});$$

$$z = L, \quad \frac{\partial T}{\partial z} = \frac{\partial C}{\partial z} = 0. \quad (2)$$

We assume that the dispersion of mass is negligible and, for a first-order activated kinetics $r = A\exp(-E/RT)C$, the system (Eqs. 1 and 2) may be rewritten in the dimensionless form as

$$\frac{\partial x}{\partial \tau}+\frac{\partial x}{\partial \xi}=Da(1-x)\exp\left(\frac{\gamma y}{\gamma+y}\right)-\alpha_C(x-x_w)=f(x,y),$$

$$Le\frac{\partial y}{\partial \tau}+\frac{\partial y}{\partial \xi}-\frac{1}{Pe}\frac{\partial^2 y}{\partial \xi^2}$$

$$=BDa(1-x)\exp\left(\frac{\gamma y}{\gamma+y}\right)-\alpha_T(y-y_w)=g(x,y). \quad (3)$$

$$\xi=0, \quad x=0, \quad \frac{1}{Pe}\frac{\partial y}{\partial \xi}=y; \quad \xi=\tilde{L}, \quad \frac{\partial y}{\partial \xi}=0. \quad (4)$$

Here the conventional notation is used

$$x=1-\frac{C}{C_{\text{in}}}, \quad y=\gamma\frac{T-T_{\text{in}}}{T_{\text{in}}}, \quad \xi=\frac{z}{z_0}, \quad \tau=\frac{tu}{z_0},$$

$$\gamma=\frac{E}{RT_{\text{in}}}, \quad B=\gamma\frac{(-\Delta H)C_{\text{in}}}{(\rho c_p)_f T_{\text{in}}}, \; Da=\frac{Az_0}{u}e^{-\gamma},$$

$$Le=\frac{(\rho c_p)_e}{(\rho c_p)_f}, \quad Pe=\frac{(\rho c_p)_f z_0 u}{k_e}, \quad \alpha_C=\frac{k_g P z_0}{u},$$

$$\alpha_T=\frac{h_T P_{z0}}{(\rho c_p) f^u} \quad (5)$$

Note that we did not use the reactor length L as the length scale, but rather an arbitrary value z_0, so that $\tilde{L}=L/z_0$ can be varied as a free parameter. The choice of $\tilde{L}$ will be discussed below. Conventional definitions of Pe and Da correspond to our $Pe\tilde{L}$ and $Da\tilde{L}$ (the symbol ''tilde'' will be omitted further). Typically, the bed heat capacity is large ($Le \gg 1$) and $Pe \gg 1$. (Note that even when Pe is around unity, the conventional definition corresponds to $Pe\tilde{L} \gg 1$.)

The solutions of the righthand side of the Eq. 3 ($f(x_s, y_s) = g(x_s, y_s) = 0$) are the asymptotic homogeneous solutions of the problem and up to three solutions may exist within a certain set of parameters. Under these conditions, we may find fronts separating different steady states.

To understand the patterns admitted by Eqs. 3 and 4, let us review the behavior of several simplified and related systems:

(I) If we ignore, for now, the heat-dispersion term, then the steady-state system

$$\frac{dx}{d\xi}=f(x,y); \qquad \frac{dy}{d\xi}=g(x,y). \quad (6)$$

is exactly the model describing the temporal dynamics of a homogeneous CSTR, in which an exothermic first-order reaction is conducted. This problem has been investigated extensively in order to map the various bifurcation diagrams and phase planes in the parameter space (Uppal et al. 1974, 1976; Guckenheimer, 1986). While reactor dynamics at the entrance zone is dictated by the feed conditions, no simple classification of the states governed by Eqs. 3 and 4 exists and the analysis of sustained motions of the CSTR (Eq. 6) is useful in describing and classifying the behavior of a long reactor. System 6 may admit, aside from the phase plane with a unique stable state (which we denote by U) or with two stable states (M), an oscillatory solution surrounding one (O) or three solutions (O_3), and multiple solutions in which the upper (or lower) one is stable (M), or surrounded by a limit-cycle (OS) or unstable and unattracting (U_3). Other phase planes, notably those due to subcritical Hopf bifurcation, may exist over narrow domains.

Each of these phase planes may be used as a starting point in investigating the full system dynamics. In a long reactor the system may approach the corresponding asymptotic state, and when two such states exist, the attained state is determined by the inlet (initial) conditions.

(II) Incorporating the dispersion-term now, while still maintaining the steady-state solution, the system is described by

$$\frac{dx}{d\xi}=f(x,y); \quad \frac{dy}{d\xi}=p; \quad \frac{dp}{d\xi}=Pe(p-g(x,y)). \quad (7)$$

The multiplicity patterns of this system are identical to those of Eq. 6, but the new term affects the dynamics. The Jacobian matrix is

$$J=\begin{pmatrix} f_x & f_y & 0 \\ 0 & 0 & 1 \\ -Peg_x & -Peg_y & Pe \end{pmatrix} \quad (8)$$

and the characteristic equation of the eigenvalues (m_i) is

$$J-mI=-m^3+m^2(f_x+Pe)-m(Pef_x+Peg_y)+detJ=0 \quad (9)$$

where $detJ=Pe(f_x g_y - g_x f_y)$. The Hopf bifurcation occurs when $m_{1,2}=\pm ik_0$

$$k_0=\left(-f_x^2-g_x f_y\right)^{1/2} \quad Pe_0=\frac{k_0^2}{f_x+g_y}, \quad (10)$$

This reduces, of course, to the Hopf bifurcation condition of the previous case when $Pe \to \infty$.

(III) Consider the full system (Eq. 3). The linear stability analysis conducted below ignores the boundary conditions; this corresponds to either a system with periodic boundary conditions or an infinitely long system which is not affected by the boundaries (a similar approach was used by Kuznetsov et al., 1997 and Andresén et al., 1999). Denoting the deviation from the basic steady-state solution $u=\{x_s, y_s\}$ as $u_1=\{x_1, y_1\}$, and linearizing the original problem, we arrive at the following system for the perturbations

$$\frac{\partial u_1}{\partial \tau}-V\frac{\partial u_1}{\partial \xi}-D\frac{\partial^2 u_1}{\partial \xi^2}=Ju_1, \quad (11)$$

where $D=diag\{0, (LePe)^{-1}\}$, and $V-diag\{1, Le^{-1}\}$ are the diffusion and convection matrices. Assuming the perturbations to be harmonic in the space variable ξ, that is $u_1=\{x_1, y_1\} \sim e^{ik\xi+\sigma\tau}$, where k is the perturbation wave number and σ is the time growth rate, and using it in Eq. 11, we obtain the dispersion relation $\mathfrak{D}(\sigma, k)=0$. It has a form of

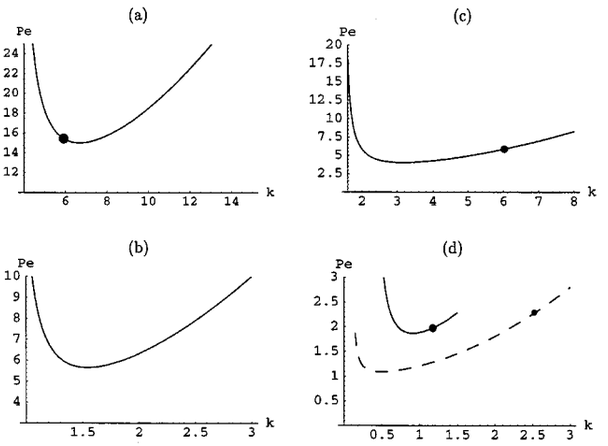

Figure 1. Typical neutral curves for various types of behavior as classified in terms of CSTR dynamics.

Parameters in (a) ($B = 16.2$, $\beta = 3$, $Da = 0.2$, as in Figure 17 in Uppal et al. (1974) correspond to a simple limit cycle, in (b) ($B = 16.2$, $\beta = 3$, $Da = 0.129$, as in Figure 20 (Uppal et al., 1974)–to a stable state surrounded by an unstable and stable limit cycles, in (c) ($B = 19$, $\beta = 3$, $Da = 0.09$, as in Figure 12 in Uppal et al. (1974))–to a globally-stable state, and in (d) ($B = 16.2$, $\beta = 3$, $Da = 0.132$, as in Figure 12 in Uppal et al. (1974))–to three unstable states surrounded by a stable limit cycle. The solid and dash lines in (*d*) correspond to the lower and upper steady-state solutions. The dot denotes the Turing point (Pe_0, k_0).

the quadratic equation with *complex* coefficients

$$\sigma^2 + (A_r + iA_i)\sigma + (N_r + iN_i) = 0, \tag{12}$$

where the coefficients are given by

$$A_r + iA_i = -\,trM, \quad N_r + iN_i = detM$$

$$M = J + ikV - k^2 D \tag{13}$$

It can be easily shown that the bifurcation condition $Re\ \sigma = 0$ is satisfied if

$$A_r^2 N_r + A_r A_i N_i = N_i^2, \tag{14}$$

while the frequency of the emerging oscillatory pattern is given by

$$\omega = Im\,\sigma = -\,N_i/A_r. \tag{15}$$

Relation 14 defines the neutral curve that may be calculated numerically for a chosen set of parameters. We used Pe as the bifurcation parameter, as it does not influence the steady-state solutions. Moreover, the stationary patterns emerging at $Pe \to \infty$ for the system (Eq. 3) correspond to the dynamic behavior of the corresponding CSTR problem. The neutral curve typically acquires a minimum (k_c, Pe_c, see Figure 1) and crossing Pe_c corresponds to an excitation of oscillatory solutions with finite k in an unbounded system moving at a constant speed.

(IV) Let us consider now the bounded system governed by the Eq. 3 with the applied boundary conditions (Eq. 4). Linear stability analysis is of limited use now as the steady state is generally not homogeneous and cannot be expressed analytically. Moreover, bifurcations in the system (Eq. 3), as we change a parameter, generically do not occur, rather, a gradual shift of patterns occur. As the simulations below demonstrate, this problem has the following unusual feature. The moving patterns predicted in the infinite region are suppressed by the boundaries, and, above, some threshold Pe *stationary patterns*, which generally do not correspond to the minimum of the neutral curve, are excited. For such patterns to emerge, we should impose a condition of zero frequency ($N_i = 0$) in addition to the relation (Eq. 14). Note that the condition $\omega = 0$ (see Eq. 15) defines a straight line in the plane (k, Pe). If both of these conditions are matched, we may determine an amplification threshold (see Figure 1). Its coordinates are identical to the Hopf bifurcation point for Eq. 7, defined by the Eq. 10.

The detailed weak nonlinear analysis of the full system that includes the derivation of the amplitude equation near the bifurcation point of an unbounded system, based on the multiscale expansion (Pismen and Rubinstein, 1999) is presented elsewhere (Nekhamkina et. al., 2000). Note that both linear and nonlinear analysis mentioned above are valid, strictly speaking, only for an unbounded system in the vicinity of a single steady state. In the bounded system this procedure should take into account the influence of the boundary conditions, which can lead to a shift of the critical wave numbers. If the system (Eq. 3) admits multiple steady-state solutions, then the dynamic behavior becomes significantly more complicated.

It should be emphasized that the CSTR model provides some information about an asymptotic behavior, when $Pe \to \infty$ and very large L. The information about the practical behavior (finite Pe and L) may be obtained only by analysis of the distributed system (Eqs. 3 and 4).

Numerical Simulations

In this section we analyze the spatiotemporal behavior of the full system (Eqs. 3 and 4) using the classification of models described above. That is, we consider some typical cases that were investigated previously for the corresponding CSTR problem by Uppal et al. (1974). Consistent with that study, we set without loss of generality $x_w = y_w = 0$ (supply conditions are similar to feed conditions), $\alpha_c = 1$ and $\alpha_T = \beta + 1$ (β is a coefficient used in Eq. 18 to describe heat transfer). In all simulations we choose $Le = 100$ and the reactor length was set $L = 10 \div 25$ in order to resolve a structure of the emerging patterns (these estimates were made according to the critical wave numbers considered in the previous chapter).

Case 1. The simplest CSTR dynamics (aside for a stable state) is one that admits an unstable steady-state solution surrounded by a stable limit cycle. The corresponding neutral curve typically acquires the form of Figure 1a and includes a bifurcation point ($Pe_0 = 15.42$, $k_0 = 5.9$. Its location close to Pe_c, the minimum of the neutral curve is coincidental.) Numerical simulations reveal that, for $Pe < Pe_c$, the homogeneous solution is established practically in the whole domain

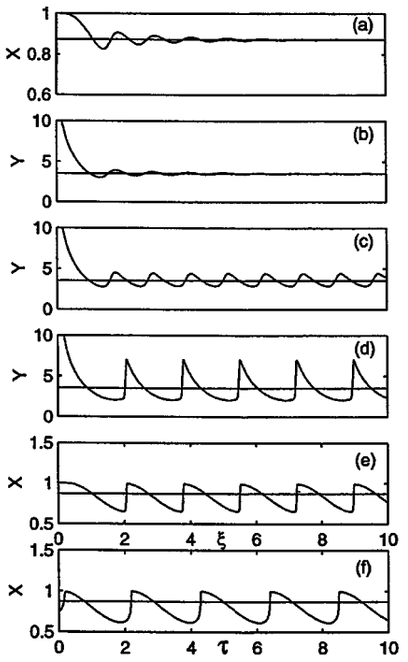

Figure 2. Steady-state profiles of the dimensionless concentration (x) (a, e) and temperature (y) for $Pe = 14$ (a, b), 20 (c), 100 (d, e) of the full system (3) and the corresponding CSTR dynamic behavior (f).

The horizontal lines show the steady-state level. (Case 1, parameters, as in Figure 1a, $L = 10$).

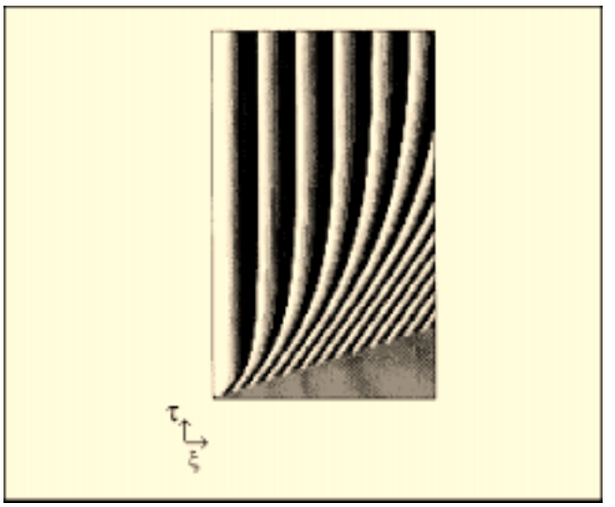

Figure 3. The transient leading to a sustained pattern starting from a homogeneous state.

Temperature is denoted as a gray scale in the time vs. space plane. (Case 1, $L = 10$, $Pe = 100$).

with some adjustment at the inlet section, due to the boundary conditions (Figures 2a and 2b). For $Pe > Pe_c$, the system exhibits transients of traveling waves: once excited, they move until they are consequently arrested near the boundaries (the dynamic behavior is illustrated by Figure 3). In the subcritical region ($Pe_c < Pe < Pe_0$) the amplitude of the wavy patterns decays along the reactor, and the profiles $y(\xi)$ and $x(\xi)$ tend to the stationary solution y_s, x_s, in similarity to the case $Pe < Pe_c$.

Stationary space-periodic patterns are established for $Pe > Pe_0$. The amplitude of these patterns varies in space but tends to some saturated value. For relatively small deviations from the bifurcation, the patterns have a harmonic form (Figure 2c) and the computed wave number is in a very good agreement with the theoretical value k_0 (Eq. 14).

With increasing $\Delta Pe \equiv Pe - Pe_0$, the amplitude of the state variables grows, the patterns become highly nonlinear (sawtooth pattern) and the wave number decreases (see Figures 2d and 2e). Numerical simulations reveal that the structure of the patterns become insensitive to the Pe number for large $Pe(> 10^3)$ and, as expected, the form of the spatial patterns completely corresponds to the dynamic behavior of the corresponding CSTR model (Figure 2f).

Case 2. When the corresponding CSTR problem admits a stable steady-state solution surrounded by an unstable limit cycle which, in turn, is enveloped by a large stable limit cycle, then the neutral curve of the full system (Figure 1b) admits a minimum but the critical amplification point is absent: $Pe_0 < 0$. The system behavior, however, is significantly more complicated than in the previous case, and cannot be predicted from the linear stability analysis in the vicinity of y_s, x_s.

For small values of Pe (< 3), the stationary solution is established. The temperature and concentration profiles are affected at the inlet by the boundary conditions and tend monotonically towards the steady state (y_s, x_s) at the exit.

With increasing Pe, local maxima of the $x(\xi)$, $y(\xi)$ profiles are formed and the hot spot oscillates within a small spatial domain (Figures 4a and 5a). If we plot $y(\xi)$ vs. $x(\xi)$, then this "spatial" phase plane shows a small meandering loop (Figure 5a (2) presents two snapshots). With increasing Pe, the limit cycle shrinks (Figure 4b, $Pe = 3.2$). Stationary patterns are established for $Pe > 3.5$. They are composed of some spatially oscillated waves in the near inlet section with transition to the asymptotic steady-state solution in the downstream section (see Figures 4c and 5b). The number of these waves increases with increasing Pe and eventually cover the whole region (Figure 5c). For high Pe, the pattern corresponding to the oscillatory CSTR solution is established.

Case 3. When the corresponding CSTR problem admits a globally-stable low-activity steady-state solution (U_3) and two unstable solutions, then the neutral curves calculated for the upper steady state (x_{s3}, y_{s3}) exhibit a local minimum and a pattern bifurcation point (Figure 1c, $Pe_{03} = 5.9$, $k_{03} = 6$). Bifurcation from the intermediate steady state (x_{s2}, y_{s2}) is not interesting, as this state is associated with a positive eigenvalue. Recall also that Pe_{03} is the Hopf bifurcation point of the ODE system (Eq. 7) and, thus, for $Pe < Pe_{03}$, this system admits two stable asymptotic states.

For $Pe < Pe_{c3}$ (~ 4.0), only stationary solutions are obtained. Depending on the initial condition, the profile of the state variables are either monotonous and strongly converging to the lower steady-state solution (x_{s1}, y_{s1}, Figure 6a (1),

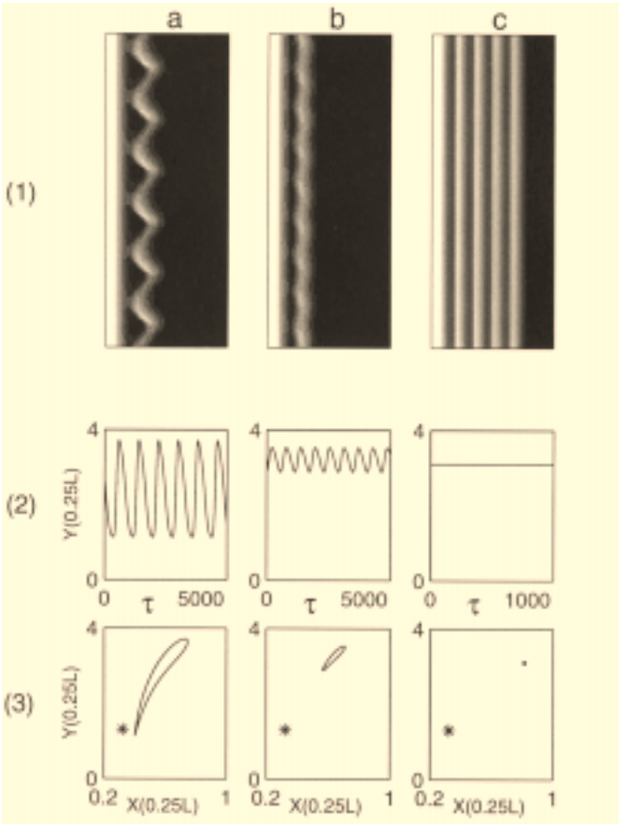

Figure 4. Effect of *Pe* on the system behavior for case 2 (parameters as in Figure 1b, $L = 10$): $Pe = 3.0$ (a), 3.2 (b), 5.0 (c).

Row 1 shows the spatiotemporal temperature patterns, row 2 exhibits the temporal behavior at $\xi = 0.25L$, and row 3 presents the phase planes for $\xi = 0.25L$. The star denotes the steady state solution.

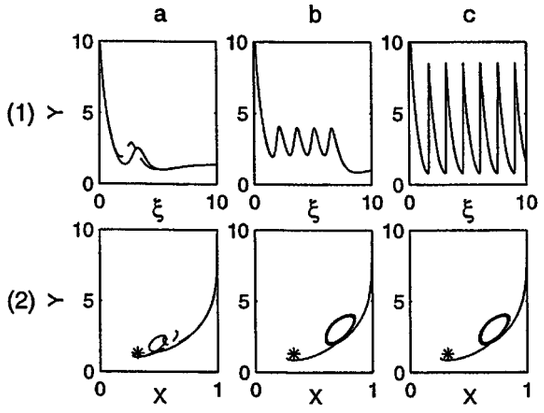

Figure 5. Transition from the moving to stationary patterns for case 2 with increasing *Pe*: $Pe = 3.0$ (a); 5.0 (b), and 100 (c).

Row 1 presents the temperature profiles along the reactor (oscillations in *a* are denoted by two snapshots expressed by solid and broken lines); row 2 presents the "spatial" phase planes ($y(\xi)$ vs. $x(\xi)$); the star denotes the steady-state solution.

broken line), or slowly waving and converging to the upper steady state (x_{s3}, y_{s3}, - Figure 6a (1), solid line). Traveling waves emerge for $Pe > Pe_{c3}$. These waves move towards the inlet and are gradually suppressed by the boundary (see Figures 6b and 6c, which exhibit two selected spatial profiles and Figures 7a (1) and 7b (1), which demonstrate the spatiotemporal behavior). The phase plane trajectories for each cross section ($y(\tau)$ vs. $x(\tau)$) aside for the inlet are single loops that envelop the upper steady state y_{s3}, x_{s3} (see Figures 6b (2) and 6c (2)). Further increase in *Pe* leads to increasing amplitude of the oscillations especially in the downstream section. For $Pe = 5.25$, a period-two solution was recorded (see Figure 7b) and a period doubling transition is expected.

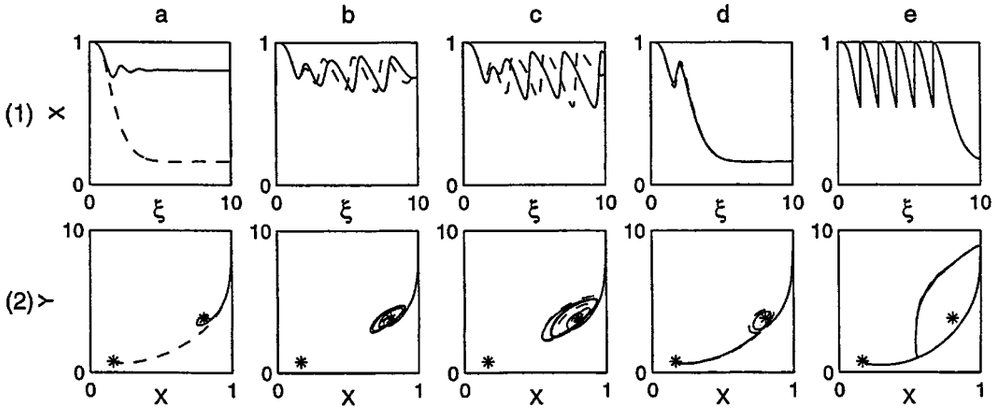

Figure 6. Transition from the almost homogeneous (a) through oscillatory wave-trains (b–d) to stationary patterns (e) for case 3 (parameters as in Figure 1c, $L = 10$) with increasing *Pe*: $Pe = 4.0$ (a), 4.5 (b), 5.25 (c), 5.27 (d), 100 (e).

Rows 1, 2 present the temperature profiles and the "spatial" phase planes as in Figure 5; (multiple solutions in (a) are denoted by solid and broken lines, oscillations in $b - d$ are denoted as in Figure 5a); the stars denote the steady-state solutions.

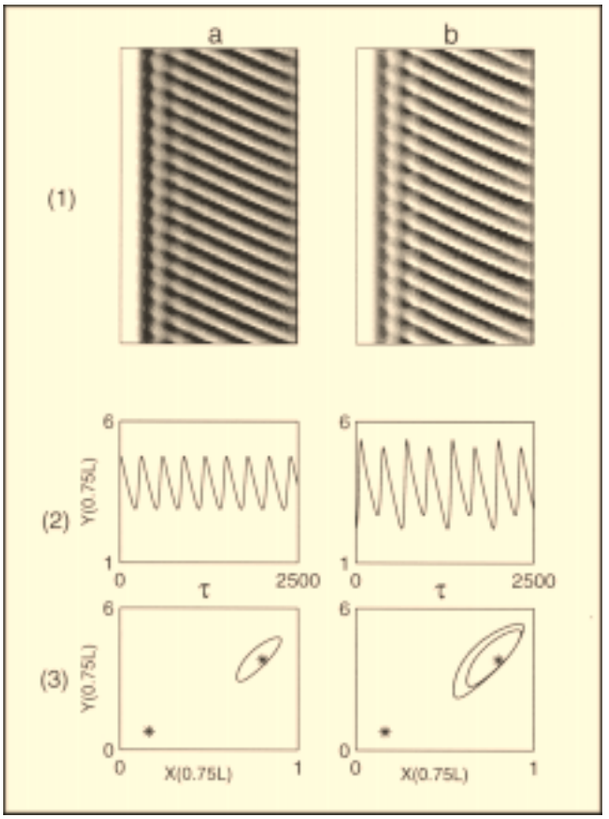

Figure 7. Effect of *Pe* on the spatiotemporal patterns for case 3: *Pe* = 4.5 ((a) period one solution), and 5.25 ((b) period-two solution).

Row 1 shows the spatiotemporal temperature patterns, row 2 exhibits the temporal behavior at $\xi = 0.75L$; and row 3 presents the phase planes for $\xi = 0.25L$; the stars denote the steady-state solutions.

A transition to the chaotic motion was not observed in this case. For $Pe \geq 5.27$, the system behavior becomes quite similar to that previously considered in case 2: First, ($Pe = 5.27$) a single breathing hot spot emerges in the near inlet section ($\xi \sim 2$), while most of the reactor ($\xi > 4$) is extinguished (Figure 6d). Further growth in *Pe* leads to the formation of the stationary patterns with an increasing number of the standing waves. In the vicinity of $Pe_{0,3}$ the numerically obtained wave number is in a very good agreement with the analytical predictions. With increasing *Pe*, the originally harmonic form of the patterns transforms, while the wave number is relatively little affected by the bifurcation parameter (Figure 6e).

Case 4. The last case to be considered corresponds to a CSTR problem which admits three unstable steady states surrounded by a single stable limit cycle. The neutral curves calculated for the lower (x_{s1}, y_{s1}) and upper (x_{s3}, y_{s3}} steady-state solutions for the full system exhibit local minima and stationary pattern bifurcation points (Figure 1d, $Pe_{01} = 1.98$, $k_{01} = 1.17$, $Pe_{03} = 2.28$, $k_{03} = 2.53$). As in case 3, for $Pe < \min (Pe_{c1}, Pe_{c3})$, only stationary solutions, depending on the initial conditions are obtained. (In the following calculations we used the intermediate steady state (x_{s2}, y_{s2}) as the initial conditions.)

In a domain which roughly lies around the two critical *Pe* the system exhibits spatiotemporal patterns (Figures 8a–8e) in which a pulse is born somewhere downstream and then moves upstream and disappears. The motion is periodic if the birthpoint of this pulse is reproduced on successive pulses, or multiperiodic or even aperiodic when it does not repeat itself. At $Pe = 1.5$, a strictly periodic motion is sustained in which a single hot spot emerges somewhere within the reactor inlet, moves upstream and disappears (Figure 8a (1)). The corresponding $y(\tau)$ vs. $x(\tau)$ phase plane exhibits a single closed loop (Figure 8a (3), cross section $\xi = 0.25L$).

Aperiodic behavior is recorded for $Pe = 2.1 \div 2.3$ (Figure 8b) and the corresponding two-dimensional (2-D) ($y(\tau)$ vs. $x(\tau)$, $\xi = 0.25$, Figure 8b (3)) or 3-D (with the addition of the derivative $dy/d\xi$ as a third coordinate - Figure 9a) phase-plane and phase-space exhibit a strange attractor.

Regular period-5 patterns are established at $Pe = 2.5$ (Figure 8c). The short waves are consequently followed by the longer waves forming a single packet which is composed of five waves. These waves are clearly evident by the temporal profile $y(0.25L, \tau)$ (Figure 8c (2)) and by the five loops in the 2-D (Figure 8c (3)) and in the 3-D (Figure 9b) phase portraits. At $Pe = 3.0$, regular moving patterns that span most of the reactor are established (Figure 8d). The period-5 pattern is maintained again in the range $3 < Pe < 4$, but unlike the lower *Pe* regimes, a single standing wave is already formed near the inlet (compare Figures 8e and 8c). We suspect that other aperiodic or multiperiodic domains may exist but, since it is not the main focus of this work, we do not try to map these domains.

The stationary patterns are established for $Pe > 5$ (Figure 8f). This value differs sufficiently from the bifurcation points, calculated for both lower and upper steady-state solutions, and the computed wave number also does not agree with any of the analytical values. With increasing *Pe*, as in the previous cases, the standing wave patterns are significantly rearranged and for $Pe > 10^4$ become quite similar to the temporary solution of the corresponding CSTR problem.

In the simulations presented above we used *Pe* as the bifurcation parameter. Below, we briefly discuss the influence of another parameter—the reactor length *L*. Note that we do not change the length scale z_0 and the other parameters are not affected. We consider case 4 with $Pe = 4$. The regular moving five-wave packet shown in Figure 8e is observed in the range $L = 20 \div 27$. For $L = 18$, a packet composed of four pulses is established. For larger values ($L > 27$), chaotic motion was observed, while for $L > 30$ a six-waves packet was established (not shown). Thus, increasing the reactor length leads to an increasing number of waves that the system holds, but we did not observe the new types of the spatio-temporal behavior.

Concluding Remarks

This work analyzes and simulates novel patterns in a simple model of a cross-flow (or membrane) reactor. While such reactors have not been applied commercially yet, the advantages of such a reactor have been outlined in the Introduction and the current extensive work into membrane reactors

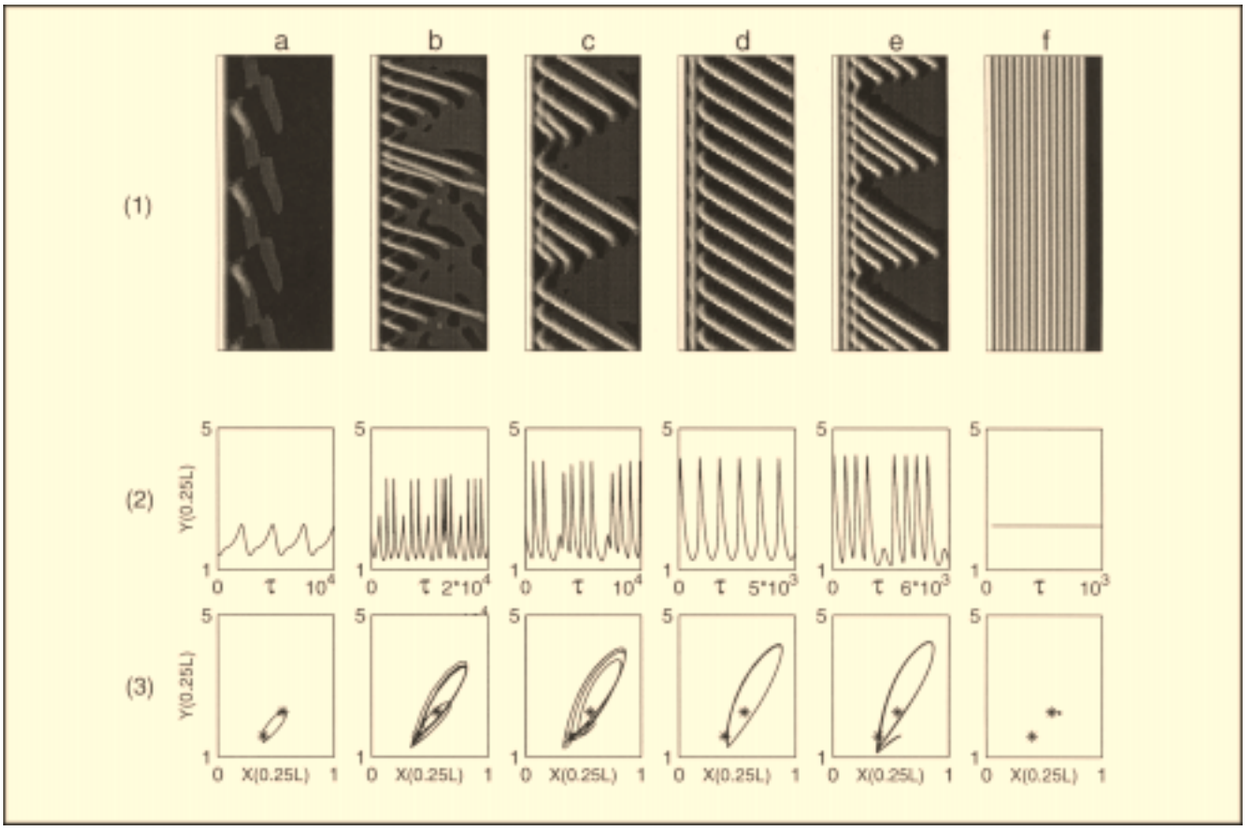

Figure 8. Effect of *Pe* on the spatiotemporal patterns for case 4 (parameters as in Figure 1d, *L* = 25).

Pe = 1.5 ((a) periodic solution with a moving hot spot), 2.1 ((b) aperiodic behavior), 2.5 ((c) period - 5 packet), 3.0 ((d) period-one patterns), 3.5 ((e)-period-5 packet), 5.0 ((f) stationary patterns). Row 1 shows the spatiotemporal temperature patterns, row 2 exhibits the temporal behavior at $\xi = 0.25$L, and row 3 presents the 2-D phase planes for $\xi = 0.25L$. The stars denote the steady-state solutions.

suggests that such processes will be applied in the future. While we have analyzed the reactor with a continuous supply of reactants, a model with finite number of supply ports will also exhibit similar behavior if their number is large enough and they are placed at the crests of the emerging wave. We still need to check the engineering implications by studying a real-case example. Such designs may be aimed at supplying oxygen to a partial oxidation reaction (see Sheintuch and Shvartsman, 1996) or coupling of endothermic dehydrogenation and exothermic oxidation reactions in a membrane reactor.

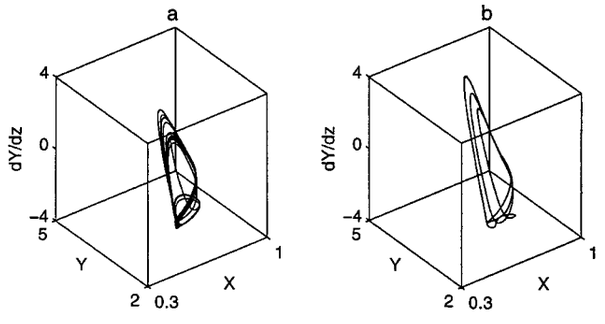

Figure 9. The 3-D ($dy/d\xi, y, x$) phase space for case 4 plotted at $\xi = 0.25L$ and different *Pe*.

Pe = 2.1 ((a), a strange attractor); 2.5 ((b), a period-5 packet).

The patterns emerge due to the interaction of reaction and convection of the activator, in contrast to Turing patterns that emerge due to competition of an activator and a fast-diffusing inhibitor in quiescent fluids. Large amplitude stationary space-periodic patterns have been simulated and analyzed for a bounded system. The linear stability analysis was performed for an unbounded system using *Pe* as a bifurcation parameter, and the analytical expression for an amplification threshold was derived. This critical value is a good predictor for stationary patterns excitation in bounded systems.

The stationary spatial behavior of the distributed system, in the limit case $Pe \to \infty$, formally correspond to the temporal dynamics of a homogeneous CSTR, which was previously comprehensively investigated. The CSTR model will not predict oscillations in catalytic systems due to the large solid heat-capacity, but that parameter will not affect the spatial

patterns presented here. For large *Pe*, stationary patterns are established in all cases. The behavior in the vicinity of the bifurcation point of the distributed system depends on the type of a phase plane that emerges for the same set of parameters in the corresponding CSTR. Only stationary patterns emerge in the distributed system for the simplest dynamics which admits an unstable steady-state solution surrounded by a stable limit cycle in a CSTR. For more complicated cases, especially for the cases when the corresponding CSTR problem admits multiple unstable steady states, both regular and aperiodic behaviors are observed in the distributed systems which obviously cannot be predicted by the linear stability analysis. The emergence of time-dependent behavior in the present thermokinetic model, in which the inhibitor (C) is fast and short-ranged, is a surprising novel phenomena, since, unlike other pattern-forming models in chemical systems, each point of the system does not exhibit oscillatory behavior. In that respect the emerging behavior is similar to cooperative phenomena observed in certain fluid-dynamics cases.

Acknowledgment

This work was supported by the Volkswagen-Stiftung Foundation. MS and BR are members of the Minerva Center of Nonlinear Dynamics. ON is partially supported by the Center for Absorption in Science, Ministry of Immigrant Absorption State of Israel.

Notation

B = dimensionless exothermicity
c_p = volume-specific heat capacity
C = key component concentration
D = axial dispersion coefficient
E = activation energy
ΔH = reaction enthalpy
Da = Damkohler number
k = thermal conductivity
Le = Lewis number
Pe = Peclet number
u = fluid velocity
t = time
T = temperature
α_T, α_C = heat and mass transfer coefficients
ϵ = bed void fraction
ρ = density

Subscripts

e = efficient value
f = fluid
in = at the inlet
s = solid
w = wall value

Literature Cited

Andresén, P., M. Bache, E. Mosekilde, G. Dewel and P. Borckmanns, "Stationary Space-Periodic Structures with Equal Diffusion Coefficients," *Phys. Rev. E*, **60**, 297 (1999).

Barto, M., and M. Sheintuch, "Excitable Waves and Spatiotemporal Patterns in a Fixed-Bed Reactor," *AIChE J.*, **40**, 120 (1994).

Hua, H., M. Mangold, A. Kienle, and E. D. Gilles, "State Profile Estimation of an Autothermal Periodic Fixed-Bed Reactor, *Chem. Eng. Sci.*, **53**, 47 (1998).

Guckenheimer, J., "Multiple Bifurcation Problems for Chemical Reactors," Physica 20D, 1 (1986).

Keren, I., and M. Sheintuch, "Modeling and Analysis of Spatiotemporal Oscillatory Patterns during CO Oxidation in the Catalytic Converter," *Chem. Eng. Sci.*, **55**, 1461 (1999).

Kuznetsov, S. P., E. Mosekilde, G. Dewel and P. Borckmans, "Absolute and Convective Instabilities in a One-Dimensional Brusselator Flow Model," *J. Chem. Phys.*, **106**, 7609 (1997).

Lauschke, G., and E. D. Gilles, "Circulation Reaction Zones in a Packed-Bed Loop Reactor," *Chem. Eng. Sci.*, **49**, 5359 (1994).

Matros, Y. Sh., and G. A. Bunimovich, "Reverse-Flow Operation in Fixed Bed Catalytic Reactors," *Catal. Rev.-Sci. Eng.*, **38**, 1 (1996).

Nekhamkina, O. A., A. A. Nepomnyashchy, B. Y. Rubinstein, and M. Sheintuch, "Nonlinear Analysis of Stationary Patterns in Convection-Reaction-Diffusion Systems," *Phys. Rev. E*, **61**, 2436 (2000).

Pismen, L. M., and B. Y. Rubinstein, "Computer Tools for Bifurcation Analysis: General Approach with Applications to Dynamical and Distributed Systems," *Int. J. Bif. Chaos*, **9**, 983 (1999).

Shvartsman, S. S., and M. Sheintuch, "One- and Two-Dimensional Spatiotemporal Patterns in a Fixed-Bed Reactor," *Chem. Eng. Sci.*, **50**, 3125 (1995).

Sheintuch, M., O. Lev, S. Mendelbaum, and B. David, "Optimal Feed Distribution in Reactors with Maximal Rate, "*Ind. Eng. Chem. Fundam.*, **25**, 228 (1986).

Sheintuch, M., and O. Nekhamkina, "Pattern Formation in Homogeneous Reactor Models," *AIChE J.*, **45**, 398 (1999).

Sheintuch, M., and O. Nekhamkina, "Pattern Formation in Homogeneous and Heterogeneous Reaction Models," *Chem. Eng. Sci.*, **54**, 4535 (1999).

Sheintuch, M., and S. Shvartsman, "Spatiotemporal Patterns in Catalytic Reactors," *AIChE J.*, **42**, 1041 (1996).

Turing, A. M., "The Chemical Basis for Morphogenesis," *Phil. Trans. R. Soc. B*, **237** (1952).

Téllez, C., M. Menéndez, and J. Santamaría, "Simulation of an Inert Membrane Reactor for the Oxidative Dehydrogenation of Butane," *Chem. Eng. Sci.*, **54**, 2917 (1999).

Uppal, A., W. H. Ray, and A. B. Poore, "On the Dynamic Behavior of Continuous Stirred Tank Reactors," *Chem. Eng. Sci.*, **29**, 967 (1974).

Uppal, A., W. H. Ray, and A. B. Poore, "The Classification of the Dynamic Behavior of Continuous Stirred Tank Reactors-Influence of Reactor Residence Time," *Chem. Eng. Sci.*, **31**, 205 (1976).

Westerterp, K. R., W. P. M. Van Swaaij, and A. A. C. M. Beenackers, *Chemical Reactor Design and Operation*, Wiley, New York (1984).

Yakhnin, V. Z., A. B. Rovinsky, and M. Menzinger, "Differential Flow Instability of the Exothermic Standard Reaction in a Tubular Cross-Flow Reactor," *Chem. Eng. Sci.*, **49**, 3257 (1994a).

Yakhnin, V. Z., A. B. Rovinsky, and M. Menzinger, "Differential-Flow-Induced Pattern Formation in the Exothermic $A \rightarrow B$ reaction," *J. Phys. Chem.*, **98**, 2116 (1994b).

Yakhnin, V. Z., A. B. Rovinsky, and M. Menzinger, "Convective Instability Induced by Differential Transport in the Tubular Packed-Bed Reactor," *Chem. Eng. Sci.*, **50**, 2853 (1995).

Manuscript received Oct. 25, 1999, and revision received Feb. 22, 2000.